Journal of Oceanology and Limnology

https://doi.org/10.1007/s00343-025-5187-9

Research Paper

Hydrochemistry and formation of shallow-buried brines in the Bankog Co Salt Lake, Xizang*

Wenjie LI[1, 2, 3], Xing LI[4, **], Qingkuan LI[1, 2, **], Qingsong ZHANG[4], Qishun FAN[1, 2], Tianyuan CHEN[1, 2], Chuntao ZHAO[1, 2], Yongsheng DU[1, 2], Yu WEI[4]

[1] *Key Laboratory of Green and High-end Utilization of Salt Lake Resources, Qinghai Institute of Salt Lakes, Chinese Academy of Sciences, Xining 810008, China*

[2] *Qinghai Provincial Key Laboratory of Geology and Environment of Salt Lakes, Xining 810008, China*

[3] *University of Chinese Academy of Sciences, Beijing 100049, China*

[4] *Sichuan Mineral Resources Exploration Group Co., Ltd., Chengdu 610051, China*

Received May 31, 2025; accepted in principle Aug. 19, 2025; accepted for publication Oct. 9, 2025

Abstract The shallow-buried brines in Bankog Co Salt Lake (BCSL) are characterized by high total dissolved solids (TDS) and K, Li, B, Br concentrations, which is apparently different from the lake waters', indicating great potential of exploitation. The hydrochemistry and formation of these shallow-buried brines are still mysterious. We collected 17 shallow-buried brine samples, and 4 lake brine samples from various locations in BCSL, and conducted elemental and D-O (deuterium, also known as heavy hydrogen and oxygen) isotopic analysis to clarify the solute sources and formation mechanisms of the shallow-buried brines. Results reveal that: (1) the shallow-buried brines are highly mineralized Na-Cl type brines, rich in Na^+, Cl^-, K^+, CO_3^{2-}, and SO_4^{2-} but poor in Ca^{2+} and Mg^{2+}. Concentrations of trace elements such as Li^+, B^{3+}, and Br^- are significantly higher than those in lake brines, and most exceed industrial mining thresholds; (2) the shallow-buried brines showed uneven spatial distribution, with high-concentration zones concentrated in the lake basin center and marginal areas significantly influenced by river dilution, providing spatial guidance for resource exploration and development; (3) D-O isotopes indicate that the brines originated from evaporated meteoric waters and possible mixing with surrounding recharge waters. Some shallow-buried brines exhibit relatively negative $\delta^{18}O$ and positive δD values, reflecting the influence of regional massive carbonate sedimentation; (4) the shallow-buried brines formation experienced a complex, multi-stage hydrochemical process. The initial meteoric waters underwent evaporation and concentration, forming high-TDS brines dominated by Na^+ and Cl^-. Carbonate precipitation reduced Ca^{2+} and Mg^{2+} concentrations, while geothermal input contributed Li^+, B^{3+}, and Br^-. Halite and glauberite dissolution-precipitation regulated Na^+, Cl^-, and SO_4^{2-} proportions. Shallow-buried brines were genetically derived from lake brines and subsequently modified by post-burial processes including groundwater mixing and mineral reactions, developing distinctive geochemical signatures while preserving their genetic connections. This study demonstrated the distinct differences between shallow-buried brines and lake brines in salt lake systems, emphasized the roles of salt mineral dissolution and precipitation, water mixing, and burial in transforming chemical compositions of the shallow-buried brines, thereby advanced the understanding of their formation and evolution.

Keyword: Bankog Co Salt Lake; shallow-buried brine; hydrochemistry; formation

1 INTRODUCTION

Brine is widely distributed in modern salt lakes and the deep layers of saline basins, with a salinity greater than 35 g/L. It is a unique liquid mineral

* Supported by the Strategic Priority Research Program of the Chinese Academy of Sciences (No. XDA0430104), the National Natural Science Foundation of China (No. U22A20573), and the Technological Innovation Research Project from Sichuan Natural Resources Investment Group Co., Ltd.

** Corresponding authors: 86014787@qq.com; liqingkuan@isl.ac.cn

resource that contains abundant common salts and strategic critical minerals, including potassium, lithium, rubidium, cesium, and strontium (Zheng et al., 2016; Liu et al., 2021a). The Qinghai-Xizang Plateau hosts more than 300 modern salt lakes, with areas larger than 1 km^2, containing substantial brine potassium, lithium, and boron resources, making them highly valuable for development (Zheng et al., 2002).

Bankog Co Salt Lake (BCSL) is located in the southern part of the Qinghai-Xizang Plateau (Fig.1a), covering an area of 140 km^2 and representing a typical continental saline lake. The lake is rich in solid salts such as hydromagnesite, mirabilite, halite, and borax, as well as brine resources rich in potassium, lithium, and boron. Previous studies have extensively investigated the mechanisms of resource enrichment and mineralization in BCSL (Zheng et al., 1989; Jiang et al., 2021; Li et al., 2022; Zhou et al., 2023), the evolution of the lake basin (Zhao et al., 2011, 2018), and the dynamics of water level changes along with their driving mechanisms (Zhao et al., 2006; Li et al., 2024, 2025), leading to a series of valuable insights. In recent years, with the accelerated warming and humidification of the Qinghai-Xizang Plateau, the water surface area of BCSL has been continuously expanding, and the lake brines are rapidly diluting (Yan et al., 2016; Li et al., 2024), posing a threat to resource development and utilization. However, large-scale shallow-buried brine resources (shallow-buried brine refers to brine or pressurized brine that is present within the pore spaces of modern salt lake mineral layers or clastic sediments, typically at depths less than or equal to 200 m) have been revealed within the salt and clastic sediments of BCSL. The shallow-buried brines are primarily distributed beneath the current lake surface, and the main aquifer lithology consists of layers of mirabilite, carbonaceous clay interbedded with mirabilite, silt, and gravel, with thicknesses ranging from 1.1 to 30.7 m and an average of approximately 12.6 m. This aquifer is covered by lake brines or clay layers and hydromagnesite layers, with the depths of 0 to 22.8 m; and laid on clay layer, with the buried depths of 4.5 to 32.8 m (Tibet Zhongxin Investment Co., Ltd., 2024). The resource reserves

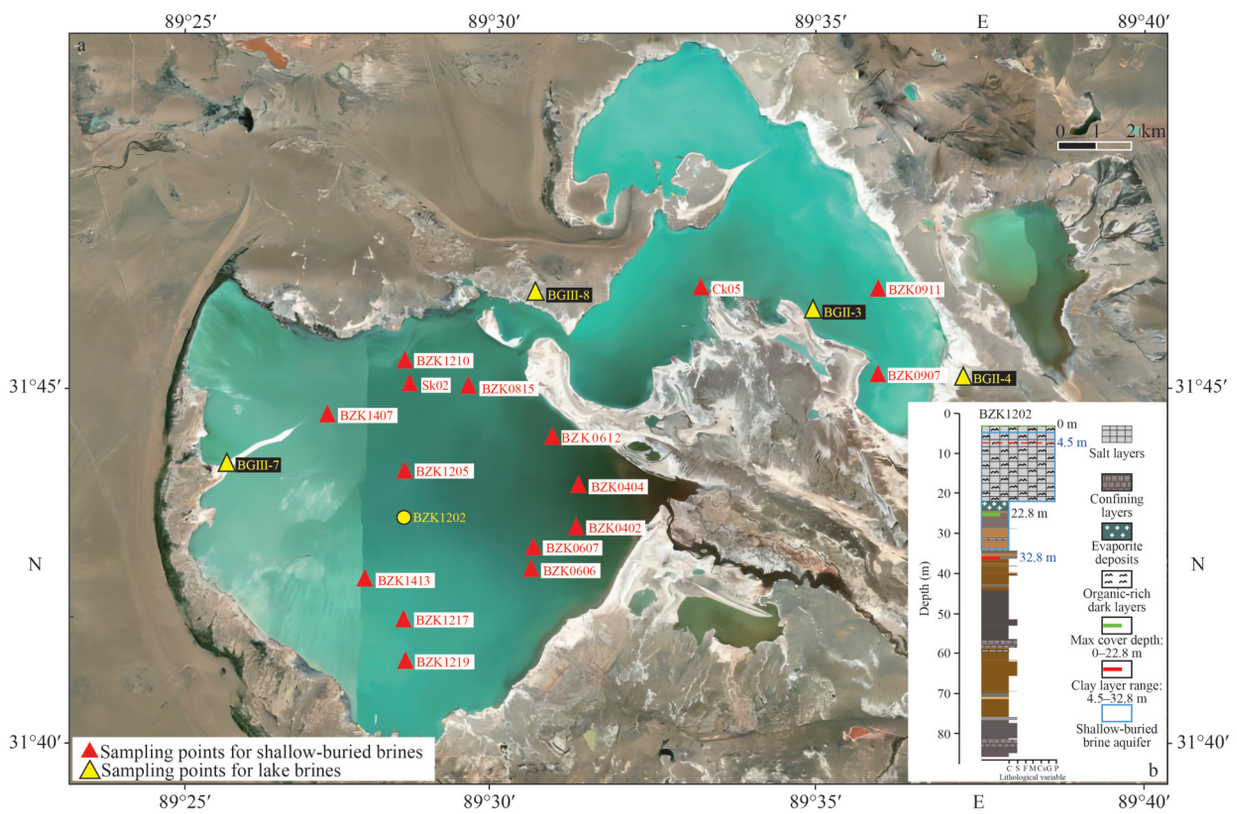

Fig.1 Distribution of brine sampling points in Bankog Co Salt Lake (BCSL)

a. distribution of sampling points for shallow-buried brines and lake brines in BCSL (the base map is derived from Jilin-1 optical satellite imagery, China nationwide coverage, 2023); b. core column of borehole BZK1202. The horizontal bar at the bottom is the lithological variable bar: C: clay/claystone; S: sand/silt; F: fine-grained sediment; M: mud/mudstone; Cs: minor clay; G: gypsum/glauberite; P: halite.

of LiCl, KCl, B_2O_3, and Br in the shallow-buried brines reach up to 1.03, 19.05, 2.71, and 0.06 million t, respectively, indicating great potential of development (Tibet Zhongxin Investment Co., Ltd., 2024). Previous studies focused on the chemical composition of the lake brines and sources of lithium and boron in the BCSL. Zheng et al. (1989) proposed that the river waters, hot/cold springs, and the neighboring Siling Co Lake waters collectively contribute amounts of lithium and boron resources to the BCSL. However, Li (2022) and Zhou et al. (2023) applied hydrochemical and boron isotopic methods to demonstrate that the lithium and boron resources in the BCSL originated from river waters and cold springs. However, the hydrochemistry and formation mechanisms of shallow-buried brines in the BCSL, and their relationship to lake brines, remain unclear. Therefore, we systematically collected the lake and shallow-buried brine samples from the BCSL and analyzed major and trace elemental compositions as well as hydrogen and oxygen isotopes (Fig.1b). On the basis of previous research outcomes, we investigated the solute sources and formation mechanisms of the shallow-buried brines. The findings in this study can contribute to a deeper understanding on the formation mechanisms of salt lake deposits.

2 GEOLOGICAL SETTING

The BCSL is located in the southern part of the endorheic Qinghai-Xizang Plateau, within the modern Siling Co-Lunpola sedimentary basin (Zhao et al., 2011, 2018). The lake basin is controlled by two sets of northwest-southeast and northeast-southwest reverse oriented faults (Zheng et al., 1989; Lü et al., 2003). Surrounding the lake basin, the exposed strata are of Mesozoic and Cenozoic age, consisting of Jurassic clastic rocks interbedded with carbonate rocks (littoral-shallow marine deposits), limestone from the Langshan Formation of the Cretaceous (shallow marine deposits), and conglomeratic sandstone, sandstone, and mudstone from the Niubao Formation of the Paleocene-Eocene (continental clastic deposits) (Zheng et al., 1989) (Fig.2).

The total area of the BCSL is about 140 km^2, consisting of three sub-basins from east to west: Lake I, Lake II, and Lake III (Bankog Co I, II, and III in Fig.2), which are separated by lake embankments formed by carbonates and clastics (Zheng et al., 2002). Lake I is a brine lake with an

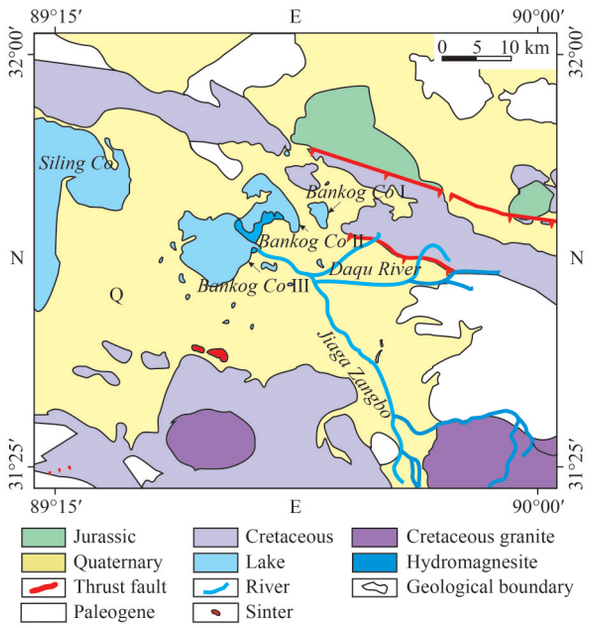

Fig.2 Simplified geological map of the BCSL (modified from Li (2022))

area of approximately 14 km^2; Lake II is a dry salt lake partially buried by eolian sands, covering about 70 km^2. Mirabilite and borates (primarily borax) deposits are found in the southern part of Lake II; Lake III has a water area in the east and mirabilite deposits in the west, with a total area of 56 km^2. In recent years, under the context of a warming and humid climate in the Qinghai-Xizang Plateau, the area of the brine lake has rapidly expanded, resulting in the connection of Lakes II and III (Liu et al., 2021b).

The hydrochemical type of the entire BCSL is carbonate type. The deposited salt minerals mainly include carbonate minerals (calcite, aragonite, hydromagnesite, magnesite, lithium magnesite, chloronatromagnesite, natronoborite, hydrated sodium carbonate, trona, and so on), sulfate minerals (mirabilite, anhydrous mirabilite, potassium mirabilite, gypsum, and so on), chloride salts (halite, hydrohalite) and borate minerals (borax, ulexite), with mirabilite, hydromagnesite and borax being abundant (Zheng et al., 2002).

The BCSL is characterized by arid cold climate, with an average annual precipitation of approximately 263 mm and an annual evaporation rate of 1 928 mm. The mean annual temperature is 0.1 °C (Zheng and Liu, 2010; Li, 2022). Clear alternation exhibits between dry and wet seasons, with 90% of annual precipitation concentrated in June–September (Yang et al., 2025). The seasonal variations

undoubtedly influence the hydrochemical evolution of the lake brines. However, the rapid decrease in total dissolved solids (TDS) and elemental concentrations of lake brines results from the increasing recharge water supply under the warmer and wetter climate on the Qinghai-Xizang Plateau (Yan et al., 2016). The primary sources of water replenishing BCSL include precipitation, river waters, and groundwaters. The southeastern part of Lake III is recharged by carbonate-rich freshwater from the Jiaga Zangbo River, the only perennial river in the basin. The drainage basin of this river covers an area of only 1 950 km^2, with an annual runoff of approximately 0.43 million m^3 (Zheng et al., 1989; Zhao et al., 2006). Additionally, the surrounding area of the lake features multiple layers of underground aquifers, with extensive cold springs emerging, particularly concentrated in the western area of Lake III and the northeastern parts of Lakes I and II. The flow rates, salinity, and chemical compositions of these spring waters are relatively stable (Zheng et al., 1989).

3 SAMPLING AND ANALYTICAL METHOD

3.1 Sampling collection

This study conducted two field investigations in the BCSL from 2023 to 2024. A total of 21 brine samples were collected, consisting of 17 shallow-buried brine samples (samples 1–17) and 4 lake brine samples (samples 21–22, 29–30), with sampling locations illustrated in Fig.1b. The lake brine samples 18–20, 23–28 are from Li (2022), and samples 31–32 are from Zheng et al. (2002).

Water samples were collected with 5-L polyethylene plastic containers. These containers were soaked in 0.1-mol/L dilute hydrochloric acid for 48 h, rinsed with ultrapure water until neutral, and then allowed to air dry in a clean workbench environment before use. During sampling, the containers were rinsed three times with waters from the sampling sites before being filled. In the field, the pH values of the waters were measured with a portable multiparameter water quality meter (SG78, Mettler Toledo). The waters were then quickly filtered through a 0.45-μm acetate fiber membrane. About 100-mL aliquot of the filtered waters were acidified to pH<2 with 6-mol/L nitric acid for cation analysis, while the remaining waters were used for anion and hydrogen-oxygen isotope composition determination.

3.2 Analytical method

The major (K^+, Na^+, Ca^{2+}, Mg^{2+}, Cl^-, SO_4^{2-}, CO_3^{2-}, HCO_3^-) and trace (Li^+, B^{3+}, Br^-) elements in all water samples were analyzed. CO_3^{2-} and HCO_3^- were determined with an automatic potentiometric titrator in accuracy of <1%. K^+, Na^+, Ca^{2+}, Mg^{2+}, Cl^-, SO_4^{2-}, and B^{3+} were analyzed using an inductively coupled plasma optical emission spectrometer (ICP-OES, ICAP6500DUO, Thermo Fisher Scientific) with the analytical error of less than 5%. Li^+ was measured with inductively coupled plasma mass spectrometer (ICP-MS, NexION 2000, PerkinElmer) in precision of <10%. Br^- was analyzed with ion chromatograph (ISC-5000+SP) in error of 2% and detection limit of 0.001 mg/L. All the tests were conducted at the Qinghai Institute of Salt Lakes, Chinese Academy of Sciences.

The hydrogen and oxygen isotopic compositions of the water samples were determined with laser liquid water isotope analyzer (IWA-45EP, LGR, USA) and performed at the Beijing Beida Zhihui Micro Structure Analysis Testing Center Co., Ltd. The precisions were $\delta D<0.3‰$ and $\delta^{18}O<0.1‰$, respectively.

4 RESULT

4.1 Major ion concentration of shallow-buried brines in the BCSL

The pH values and elemental compositions of the shallow-buried brines in BCSL are presented in Supplementary Table S1. The pH values of the shallow-buried brines range from 8.55 to 9.77, which is alkaline. The TDS range from 58.5 to 325.3 g/L, on average of 175.1 g/L.

The major ions (K^+, Na^+, Ca^{2+}, Mg^{2+}, Cl^-, SO_4^{2-}, CO_3^{2-}, HCO_3^-) in shallow-buried brines exhibit similar distribution characteristics (Fig.3). The anions and cations are in a state of equilibrium (Supplementary Fig.S1). Sodium (19 871–106 586 mg/L, on average of 59 248 mg/L) and Cl (16 436 to 139 295 mg/L, on average of 62 481 mg/L) ions are the most important cation and anion in the brines, followed by SO_4^{2-}, CO_3^{2-}, and K^+, on average concentrations of 59 248, 17 464, and 11 288 mg/L, respectively. Ca^{2+} and Mg^{2+} concentrations are lower, averaging 6 and 86 mg/L, respectively, and Mg^{2+} showed considerable variability (2–919 mg/L in range).

The major ion compositions of lake brines differ from those of shallow-buried brines (Fig.3; Li, 2022). The highest concentration in lake brines is SO_4^{2-} (average 60 807 mg/L), followed by Na^+

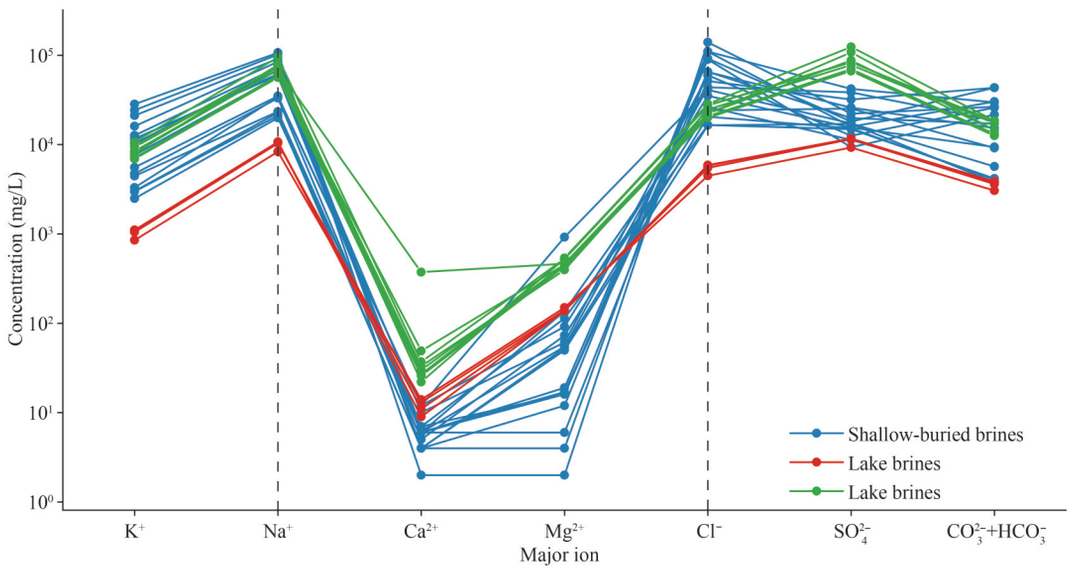

Fig.3 Distribution of major ion concentrations of shallow-buried brines and lake brines in the BCSL

Shallow-buried brines data from this study; lake brines data (red circles) from this study; lake brines data (green circles) from Li (2022).

(52 022 mg/L), Cl^- (21 802 mg/L), K^+ (5 713 mg/L), HCO_3^- (6 053 mg/L), CO_3^{2-} (5 713 mg/L), Mg^{2+} (329 mg/L), and Ca^{2+} (545 mg/L). Figure 3 reveals that the lake brines of this study (red lines) showed consistently lower ion concentrations than those of Li (2022) (green lines), with an approximately parallel downward shift across all major ions. This parallel displacement indicates systematic dilution rather than selective ion removal, suggesting that the lake brines have undergone uniform dilution since the sampling period in Li (2022). This observation aligns with the documented expansion of the lake surface area and increased freshwater input due to enhanced precipitation and glacial melt in recent years. In addition, the ion concentrations across the shallow-buried brines (blue lines) are generally homogeneous. The compositions vary in parallel along the vertical axis, suggesting a dilution-concentration trend, and implying some degree of ionic proportionality. Some variation, particularly in the anions, notably chloride, is also visible, as demonstrated by the crossing of lines between magnesium (left side) and sulfates/carbonates (right side). The ionic composition profiles of lake brines (red and green lines) do not cross, suggesting more uniform relative proportions across the lake brine samples.

4.2 Trace elemental concentration of shallow-buried brines in the BCSL

As shown in Fig.4, B^{3+} concentration of the shallow-buried brines in the BCSL was measured 183.5–1 601.6 mg/L in range, on average of 870.5 mg/L, which exceeded the industrial extraction threshold of 300 mg/L. The average concentration of Li^+ was 217.3 mg/L, which, although lower than that of B^{3+}, is still significantly higher than the industrial extraction standard of 24.6 mg/L, indicating great potential for development. Br^- concentrations in the shallow-buried brines averaged 38.30 mg/L, close to the average (41.1 mg/L) of Qinghai-Xizang Plateau salt lakes (Yu et al., 2024). Similar to variations in the TDS and major ionic concentrations, trace elements also varied significantly among different shallow-buried brine samples. Nevertheless, the distribution characteristics of Li, B, Br ions are comparable, suggesting that their sources and accumulation processes are similar. The average concentrations of B^{3+}, Li^+, and Br^- in the lake brines are 93.37, 20.26, and 1.88 mg/L, respectively, which are significantly lower than those in the shallow-buried brines.

4.3 D-O isotope of shallow-buried brines in the BCSL

The stable isotopic compositions of hydrogen and oxygen (Fig.5) indicate that the $\delta^{18}O$ and δD values of the shallow-buried brines in the BCSL scattered, with $\delta^{18}O$ ranging from -10.66‰ to -4.66‰ and δD varying between -81.62‰ and -60.19‰. This indicates different origin of the shallow-buried brines. In contrast, the $\delta^{18}O$ and δD values of the lake brines in the BCSL are comparable, with $\delta^{18}O$ values ranging from -5.24‰ to -4.76‰ and δD values fluctuating between -58.88‰ and -58.26‰. The D-O isotopes of the shallow-buried

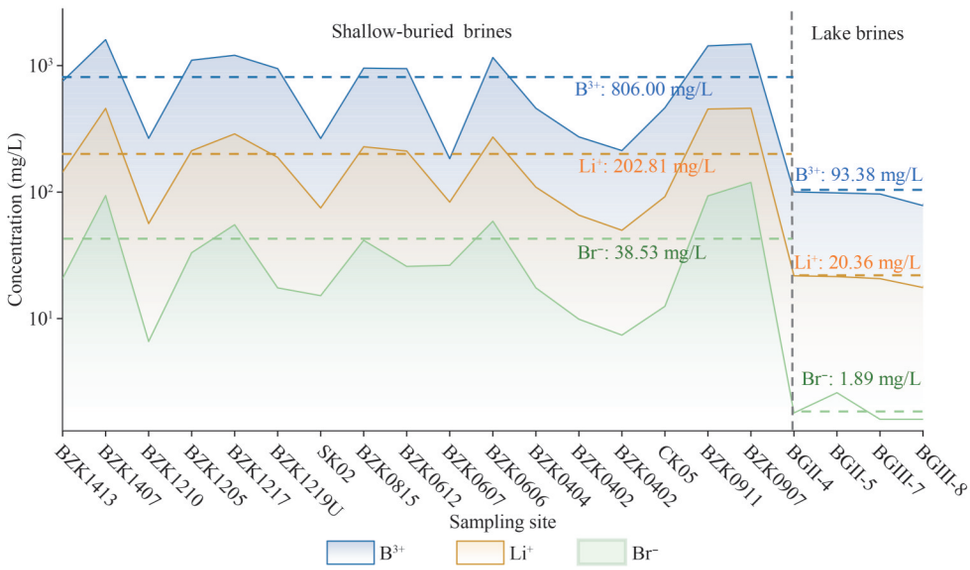

Fig.4 Distribution of trace elemental concentrations of shallow-buried brines and lake brines in the BCSL

Samples are arranged sequentially from west to east.

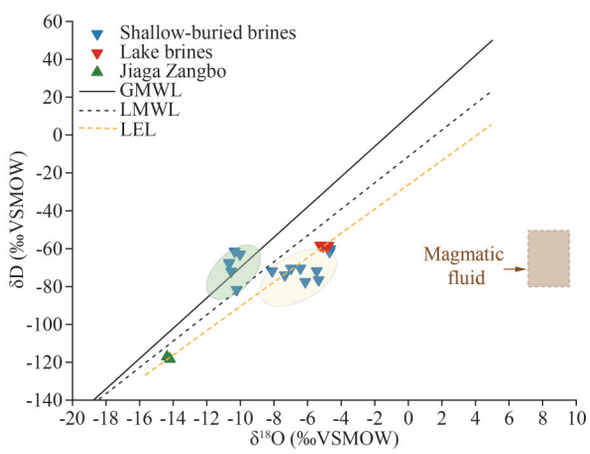

Fig.5 Characteristics of D-O isotopes distribution of brines in the BCSL

GMWL: global meteoric water line (Craig, 1961); LMWL: local meteoric water line (Yang et al., 2021); LEL: local evaporative line; VSMOW: Vienna Standard Mean Ocean Water; magmatic fluid (Taylor, 1974); green and yellow shaded fields: the isotopic clusters scattered on either side of the LMWL.

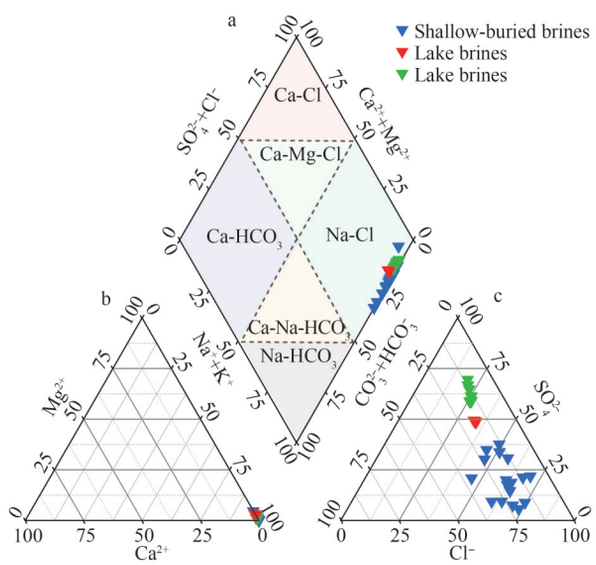

Fig.6 Piper diagram of hydrochemistry for shallow-buried brines and lake brines in the BCSL

Shallow-buried brines data from this study; lake brines data (red triangles) from this study; lake brines data (green triangles) from Li (2022); units used in the diagrams are specified as meq/L; colored fields in the diamond-shaped diagram represent different water chemistry types.

brines are generally lower than those of the lake brines, suggesting that, in addition to evaporation, other hydrological processes influenced the formation of shallow-buried brines.

5 DISCUSSION

5.1 Hydrochemical characteristic of shallow-buried brines

The Piper diagrams (Fig.6) for the shallow-buried brines and lake brines from the BCSL indicate that both types of brines belong to the Na-Cl type (Fig.6a). Both brine types exhibit high Na^++K^+ and low Ca^{2+}-Mg^{2+} characteristics (Fig.6b). Compared to the lake brines, the shallow-buried brine has a Cl^- milliequivalent proportion exceeding 45% (Fig.6c), while the proportions of SO_4^{2-} (<38%) and CO_3^{2-}+HCO_3^- (<34%) are relatively low, indicating that this type of brines have been altered during burial processes, such as salt dissolution, mineral precipitation, and different water mixing.

5.2 Planar distribution of K, Li, B, Br resources of shallow-buried brines

Shallow-buried brines are rich in valuable elements such as K^+, Li^+, B^{3+}, and Br^-. Figure 7 illustrates horizontal variations in the K^+, Li^+, B^{3+}, and Br^- concentrations across different shallow-buried brines. The highest K^+ concentrations were found in samples BZK1407, BZK0911, and BZK0907, ranging 21 208–28 370 mg/L. Meanwhile, the B^{3+}, Li^+, and Br^- concentrations in these boreholes were also notably elevated, ranging 1 358.5–1 601.6, 453.8–460.2, and 93.2–119.4 mg/L, respectively. The highest concentrations of these ions are observed in the most saline samples. (TDS vs. K=0.92; TDS vs. Li=0.88; TDS vs. B=0.79; TDS vs. Br=0.77). The strong correlations among the K^+, Li^+, B^{3+}, and Br^- resource elements suggest a common source of these ions (K vs. Li=0.95, Li vs. B=0.84, K vs. B=0.85, K vs. Br=0.81, Li vs. Br=0.84, B vs. Br=0.70) (Fig.8). Conversely, concentrations of these resource elements were generally low in boreholes BZK0402, BZK1210, BZK0607, SK02, and CK05.

The spatial distribution pattern can be identified in the shallow-buried brines. Higher ion concentrations and salinities are predominantly observed in the southern part of Lake II and the central region of Lake III, where TDS values exceed 300 g/L. Toward the lake margins, both salinity and ion concentrations show a decreasing trend. Particularly in the southeastern area of Lake III, where the Jiaga Zangbo River enters the lake, the lowest salinity samples (BZK0402) are observed, with TDS values below 60 g/L. Diluted water from river inflow clearly influences the southeastern area, while the dissolution and precipitation of evaporite layers (including halite, mirabilite, and borax) control ion concentrations in different zones. Additionally, potential geothermal contributions, as evidenced by elevated Li^+, B^{3+}, and Br^- concentrations in certain areas, may locally enhance mineralization. The variable degrees of hydraulic connectivity between different areas, combined with these multiple controlling factors, result in the observed heterogeneous distribution of the shallow-buried brines, indicating complex formation and evolution processes.

5.3 Water source indicated by D-O isotopes

As shown in Fig.5, the shallow-buried brines and lake brines in the BCSL plot in different areas. The $\delta^{18}O$ values of the lake brines are higher than those

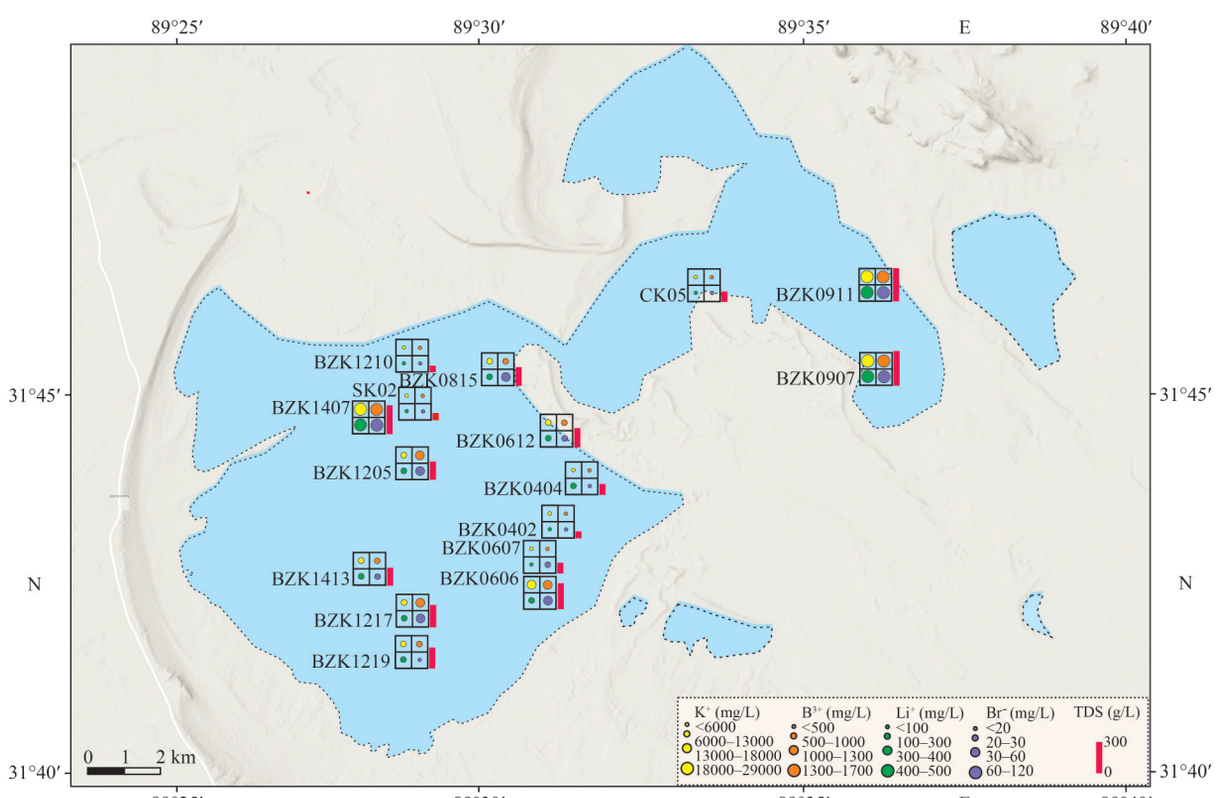

Fig.7 Planar distribution of K, Li, B, Br resource elements of shallow-buried brines

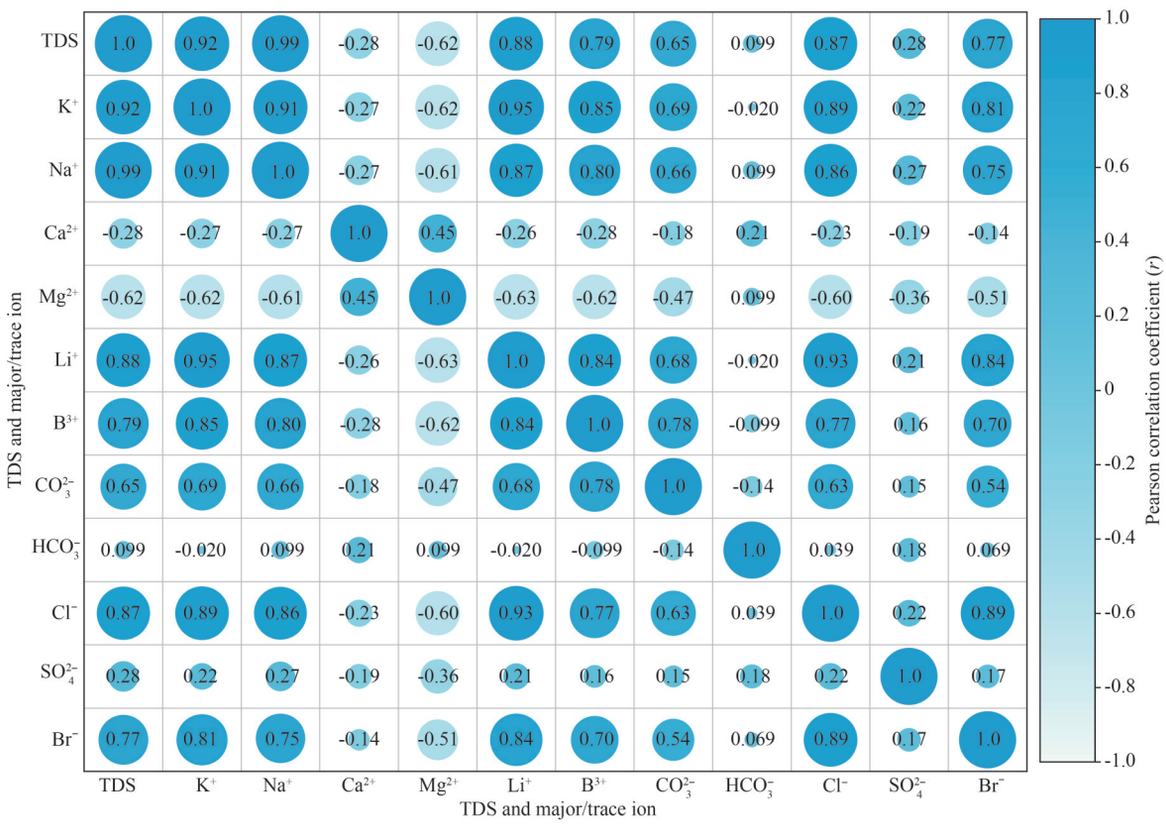

Fig.8 Pearson correlation coefficients between TDS and major/trace ions in shallow-buried brines (*n*=17)

of the shallow-buried brines, with a corresponding increase in δD values. The high D-O isotopes, coupled with lower deuterium excess values (-20.0 to -16.3), suggest that the lake brines have experienced strong evaporation. In the arid environment of the plateau, continuous evaporation of water bodies leads to the loss of lighter isotopes (such as ^{1}H and ^{16}O), resulting in elevated hydrogen and oxygen isotope values in the remaining lake waters. D-O isotopes of the evaporated brines deviate from the Global Meteoric Water Line (GMWL; Craig, 1961) and the Local Meteoric Water Line (LMWL; Yang et al., 2021). Although the lake waters receive external inputs from precipitation and snowmelt, the strong evaporation is the primary driving factor for the enrichment of heavy isotopes in the lake brines.

Most $\delta^{18}O$ and δD values of the shallow-buried brines are located along the evaporation line fitted by regional river waters and lake brines ($\delta D=6.353\times\delta^{18}O-26.900$), indicating that the shallow-buried brines are derived from meteoric waters and experienced strong evaporation. Moreover, the hydrogen and oxygen isotopes of the shallow-buried brines are slightly lower than those of the lake brines, which may be caused by several possibilities. First, this may indicate a lower degree of evaporation concentration compared to the surface lake brines. Second, it may reflect mixing with surrounding recharge waters. Third, and importantly, these isotopic signatures could result from recharge waters infiltrating into the subsurface before reaching the salt lake surface, resulting in reduced evaporative concentration. Some shallow-buried brines exhibit distinctly negative oxygen isotopes or positive hydrogen isotopes, which may be related to the large-scale deposition of carbonate minerals (such as hydromagnesite, calcite, dolomite, and natron) in the region. The deposition of carbonate minerals can lead to a decrease in the oxygen isotopes and an increase in the hydrogen isotopes of the lake waters (Stewart, 1974; Horita and Gat, 1989; Kim et al., 2007).

5.4 Solute source of the shallow-buried brines

5.4.1 Ion correlation and cluster analysis

Pearson correlation analysis can reflect the correlations among different ions in water bodies and provide valuable information regarding the sources of these ions (Fig.8). The total dissolved

solids (TDS) of the shallow-buried brines show significant positive correlations with the major ions Na^+, K^+, CO_3^{2-}, and Cl^- (correlation coefficients ranging from 0.65 to 0.99), particularly with Na^+, which has a correlation coefficient of 0.99. The correlation coefficients among Na^+, K^+, and Cl^- range from 0.86 to 0.91, suggesting that these ions have similar geochemical behaviors and become increasingly concentrated along with evaporation process. Previous studies indicate that the BCSL primarily receives inflow from the Jiaga Zangbo River and surrounding cold springs; moreover, atmospheric precipitation, silicate weathering, and evaporite dissolution collectively contribute to the sources of Na^+, K^+, and Cl^- (Zhou et al., 2023). Additionally, trace elements such as Li^+, B^{3+}, and Br^- exhibit strong correlations with TDS, and the correlations among Li^+, B^{3+}, and Br^- are notably good, suggesting that these elements share similar sources and geochemical behaviors. The sources of Li^+, B^{3+}, and Br^- in the salt lakes on the Qinghai-Xizang Plateau are closely related to the hot springs (Jiang, 2020; Wang et al., 2020; Liu et al., 2023; Niu et al., 2023; Shi et al., 2024; Yu et al., 2024). During the field investigation, no modern hot springs were identified in the drainage area; however, large-scale spring sinters were observed in the southern part of the lake area. Previous studies have reported that these hot springs possess exceptionally high concentrations of Li^+, B^{3+}, and Br^- (Zheng et al., 1989). This observation of geothermal spring deposits aligns remarkably well with the elevated ion concentrations observed in the southern part of Lake II, as shown in Fig.6. It can be speculated that during geological history, these hot springs may have supplied significant amounts of Li^+, B^{3+}, and Br^- to the BCSL. The sulfate ion (SO_4^{2-}) shows no significant correlation with other ions, suggesting multiple factors controlling its concentration in the shallow-buried brines. Firstly, different sulfate sources may contribute to the system, including dissolution of sulfate-bearing evaporites (such as gypsum and mirabilite), oxidation of sulfide minerals in surrounding rocks, and potential input from deep geothermal fluids. Secondly, sulfate concentrations are influenced by mineral precipitation processes, particularly the formation of gypsum ($CaSO_4 \cdot 2H_2O$) and mirabilite ($Na_2SO_4 \cdot 10H_2O$) under various temperature and salinity conditions. Thirdly, bacterial sulfate reduction in anoxic zones of the shallow-buried brine system may selectively remove sulfate, further decoupling its behavior from other conservative ions. Moderate correlations were observed between Mg^{2+} and Ca^{2+} (0.45), while both ions exhibited weak negative correlations with other ions (ranging from 0.099 to -0.62). This suggests that Mg^{2+} and Ca^{2+} share similar and distinct evolutionary behaviors in the brines. As divalent cations, Mg^{2+} and Ca^{2+} readily combine with carbonate ions (CO_3^{2-}, HCO_3^-) during the evolution of the water bodies, leading to the formation of carbonate precipitates and influencing their enrichment behavior in the brines.

To further analyze the source of solutes in shallow-buried brines, a hierarchical clustering analysis (R-type) was conducted on the chemical compositions of brine samples from the BCSL (Fig.9). The results of the R-type clustering analysis indicated that the chemical components of the shallow-buried brines were categorized into four distinct groups, consistent with the findings from the ion correlation analysis. Ca^{2+} and Mg^{2+} clustered closely together, suggesting similar geochemical behaviors during the evolution of the brines, which were influenced by the precipitation of carbonate minerals. Na^+, K^+, Cl^-, Li^+, B^{3+}, and Br^- formed a separate cluster, reflecting their common source of solutes and similar hydrochemical behaviors. Conversely, SO_4^{2-} was isolated in its own cluster, indicating a unique source and geochemical behavior distinct from other ions.

5.4.2 Ion ratio analysis

The Na and Cl weight ratio (rNa/rCl) serves as an important indicator of brine evolution process. As illustrated in Fig.10a, the shallow-buried brines show lower rNa/rCl compared to lake brines,

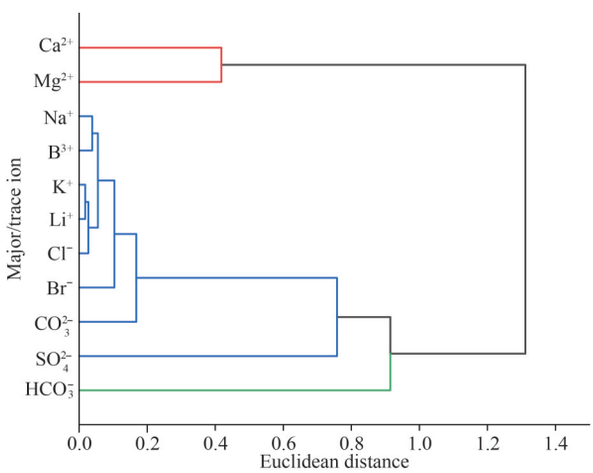

Fig.9 Q-mode cluster analysis of major/trace ions in shallow-buried brines (*n*=17)

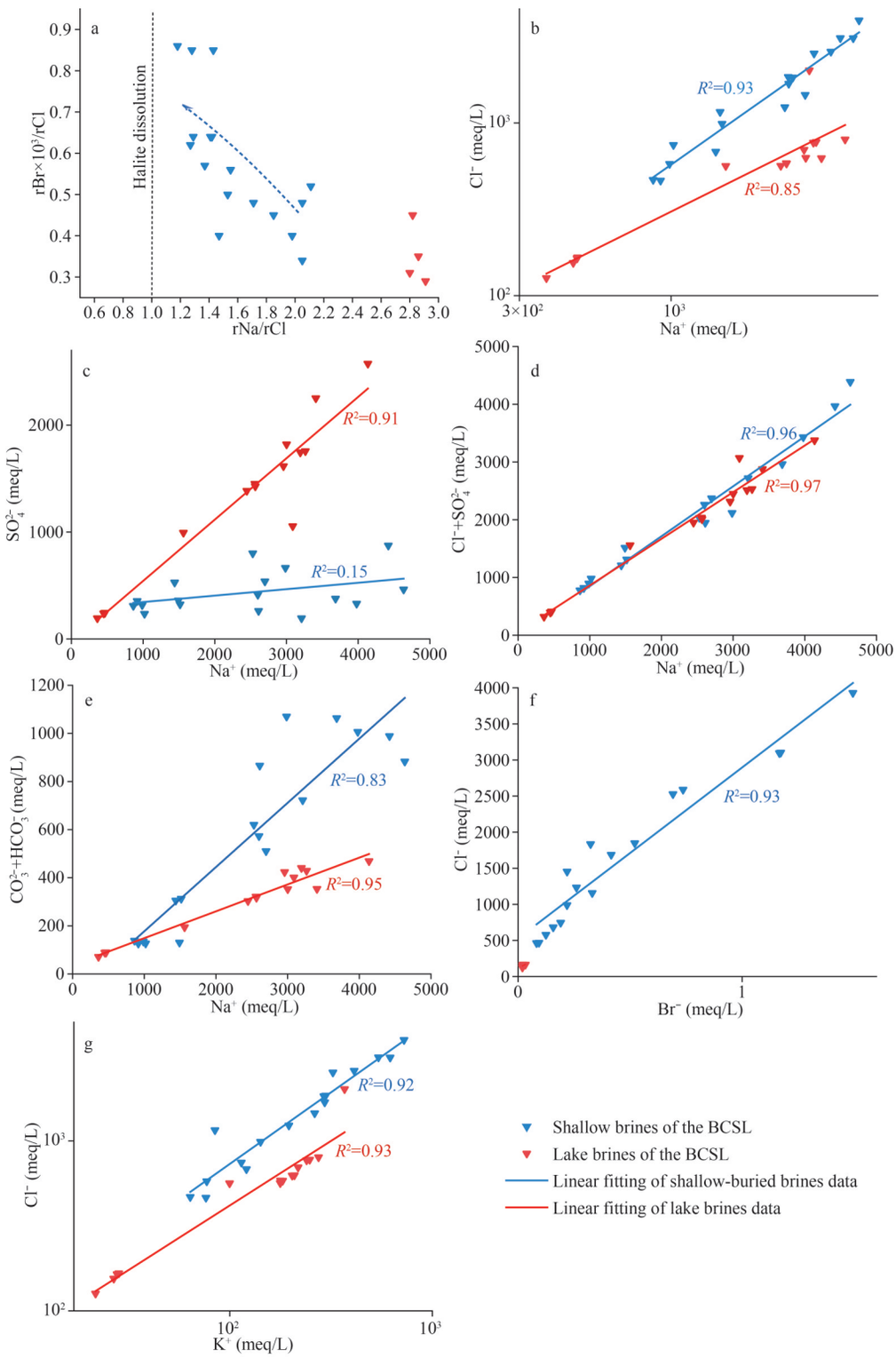

Fig.10 Relationships between major ions in the brines of BCSL

Shallow-buried brines data are from this study; lake brines data from this study, Zheng et al. (2002), and Li (2022).

approaching the 1∶1 line for halite dissolution, implying that halite dissolution plays a significant role in the formation of shallow-buried brines. Furthermore, as shown in Fig.10a, there is a strong correlation (0.93) between Na^+ and Cl^- ions in shallow-buried brines. Notably, at equivalent concentrations of sodium or

potassium ions, the Cl^- concentrations in shallow-buried brines are significantly higher than that in lake brines (Fig.10b & g), further suggesting that the dissolution of halite contributes considerable Na^+ and Cl^- to the brines. Halite in the shallow-buried brines are unsaturated (Fig.11), supporting the continuous dissolution of halite into the brines.

The decrease in the rNa/rCl ratios in shallow-buried brines may be also related to the precipitation of sodium salts, besides halite. Within the lake area, mirabilite ($Na_2SO_4 \cdot 10H_2O$) deposits are widely distributed, and supersaturated in some shallow-buried brines, suggesting that sodium in the shallow-buried brines may precipitate in the form of mirabilite. The precipitation of mirabilite reduces the Na^+ and SO_4^{2-} concentrations of the brines. Thus, there is a strong positive correlation between Na^+ and SO_4^{2-} in the lake brines, reflecting their co-evolution through evaporative concentration. However, the relationship between Na^+ and SO_4^{2-} in shallow-buried brines is more complex, resulting in weak or no correlation between these ions (Fig.10c). This decoupling arises from multiple processes: (1) differential dissolution of evaporite minerals, where halite or sodium carbonate salts release Na^+ without SO_4^{2-} while gypsum or glaserite provides SO_4^{2-} without Na^{2+}; (2) temperature-controlled mirabilite precipitation-dissolution cycles that selectively affect SO_4^{2-} concentrations; (3) variable recharge water inputs with distinct chemical compositions, as evidenced by lower TDS near the Jiaga Zangbo River inflow, creating spatial variations in ion ratios; (4) brine-sediment interactions including ion exchange with clay minerals; and (5) complex multi-component salt equilibria where competing precipitation reactions modify ion ratios. These processes work simultaneously across different zones of the shallow-buried brine system, producing the observed decoupling between Na^+ and SO_4^{2-} (Fig.10c). Both shallow-buried brines and lake brines exhibit a strong positive correlation between Na^+ and $Cl^-+SO_4^{2-}$ (Fig.10d), indicating that variations in Na^+, Cl^-, and SO_4^{2-} concentrations in shallow-buried brines are primarily related to the dissolution or precipitation of halite and mirabilite (Supplementary Fig.S2).

Some shallow-buried brines are characterized by low TDS. These brines may be influenced by the recharge of surrounding freshwaters or lake brines, causing the depletion of H-O isotopes in some water bodies.

During the dissolution of halite, the expected bromine-to-chlorine ratio should decrease. However, compared to lake brines, the bromine contents and the rBr/rCl ratios in most shallow-buried brines increased (Fig.10a, f). This anomalous phenomenon suggests that there may be other sources of Br^- in the shallow-buried brines. Previous studies reported that Br^- may become fixed in clay minerals or organic matters during lake sedimentation (Zhang, 1987; Cheng et al., 2008). Under burial conditions, Br^- can be released into the shallow-buried brines during the organic matter decomposition and desorption of clay. As shown in Fig.10a, the lower the Na/Cl ratios, the higher the Br/Cl ratios, suggesting that dissolution of halite resulting from

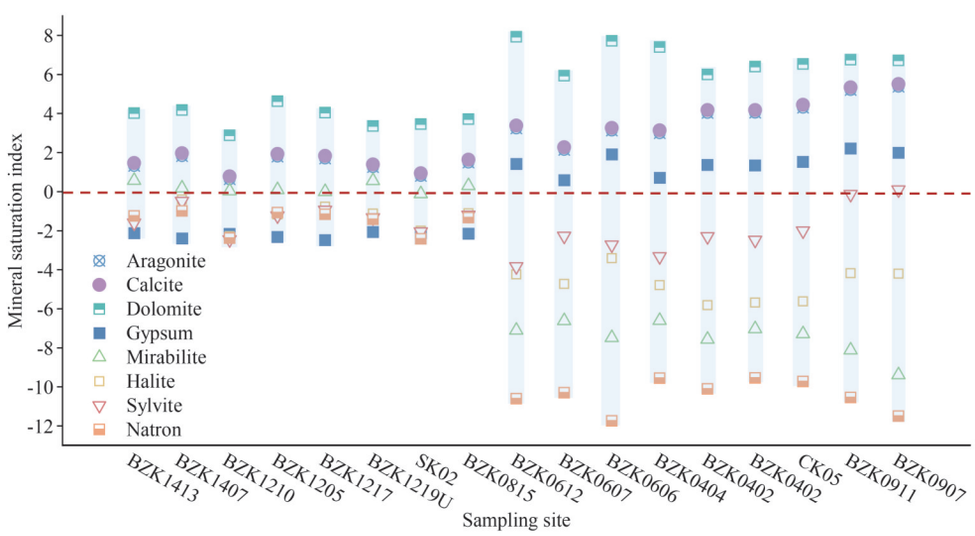

Fig.11 Schematic diagram of mineral saturation of shallow-buried brine samples

Samples are arranged sequentially from west to east.

the supply of diluted waters could favor the release of Br from the sediments.

The $CO_3^{2-}+HCO_3^-$ concentrations in the shallow-buried brines are significantly higher than that in the lake brines (Fig.10e). This carbonate enrichment can be attributed to multiple sources and processes in the basin. First, the reduced evaporation rates in the subsurface environment, as indicated by the lighter isotopic signatures discussed earlier, limit CO_2 degassing and thus preserve higher carbonate alkalinity compared to surface brines. Secondly, the geological setting of the Bankog Co basin provided significant carbonate sources through weathering processes. The surrounding catchment contained Mesozoic marine carbonate formations and Paleozoic limestone sequences that contributed dissolved carbonates through chemical weathering (Yin and Harrison, 2000; Kapp et al., 2005). Thirdly, the dissolution of lacustrine carbonate minerals such as nahcolite ($NaHCO_3$), trona ($Na_3H(CO_3)_2\cdot 2H_2O$), and natron ($Na_2CO_3\cdot 10H_2O$) within the aquifer sediments provided an additional internal source of carbonates. These authigenic carbonate minerals, formed during previous lake level fluctuations and evaporative cycles, are well-documented in Xizang salt lakes (Zheng et al., 1989; Zheng et al., 2009).

Both shallow-buried brines and lake brines exhibit a strong positive correlation between Li^+ and B^{3+} (Fig.12), indicating a common source. However, the B^{3+} concentration in shallow-buried brines is significantly lower than that in lake brines, which may be attributed to the precipitation of boron-bearing minerals (e.g., borax). The stable hydrogeological

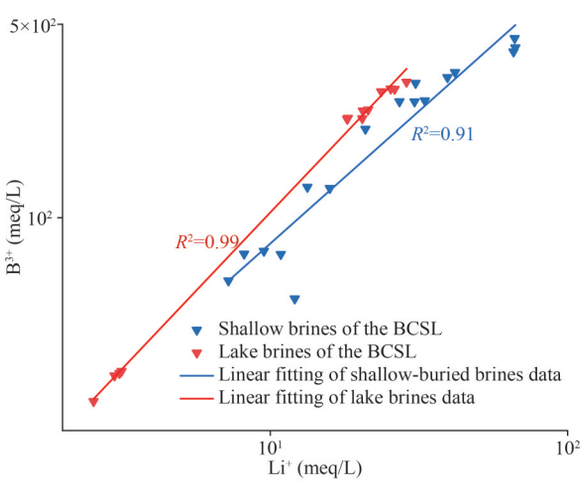

Fig.12 Relationships between Li^+ and B^{3+} in the brines of BCSL

Shallow-buried brines data from this study; lake brines data from this study and Li (2022).

conditions and high boron concentration of shallow buried brines facilitate the deposition of borate minerals (Zhang, 1987).

5.5 Formation model of the shallow-buried brines in the BCSL

The formation mechanism of the shallow-buried brines in BCSL can be described as a complex and multi-stage hydrochemical process (Fig.13). Initially, the water source of the brines was meteoric waters. The meteoric waters supplied considerable solutes to the lakes through rivers and cold springs. Geothermal waters also contributed critical elements to the lake. Next, these waters had undergone prolonged evaporation within the lake basin, resulting in high TDS of the brines. During the evaporation process, major Na, K, Cl, SO_4 and trace B, Li, Br ions concentrated in the brines, while Ca^{2+} and Mg^{2+} in the brines precipitated in the form of carbonate minerals such as calcite, aragonite, and hydromagnesite. As evaporation continues, amounts of mirabilite and halite precipitated, and brines occurred in the pores of the salts, and further were covered by clastic sediments or lake brines. Later, the shallow-buried brines experienced alteration processes during the burial process. The dissolution and precipitation of halite and mirabilite dynamically regulated the concentrations of Na^+, Cl^-, and SO_4^{2-} in the shallow-buried brines. Some shallow-buried brines exhibited significantly low TDS due to the mixing of diluted waters, suggesting strong hydraulic connection between the shallow-buried brines and the recharge waters.

The increased concentrations of bromine and the bromine-to-chlorine ratio in the shallow-buried brines might be associated with the decomposition of organic matter during burial and the leaching effects of the water, leading to the release of Br^- into the brine.

The shallow-buried brines and surface lake brines exhibited a close genetic relationship. While retaining their genetic connection to the parent surface brines, they have developed distinct geochemical characteristics through post-burial modifications including groundwater mixing, mineral dissolution-precipitation, and water-rock interactions.

6 CONCLUSION

The shallow-buried brines in the BCSL have significant potential for development. This study conducts a detailed investigation into the

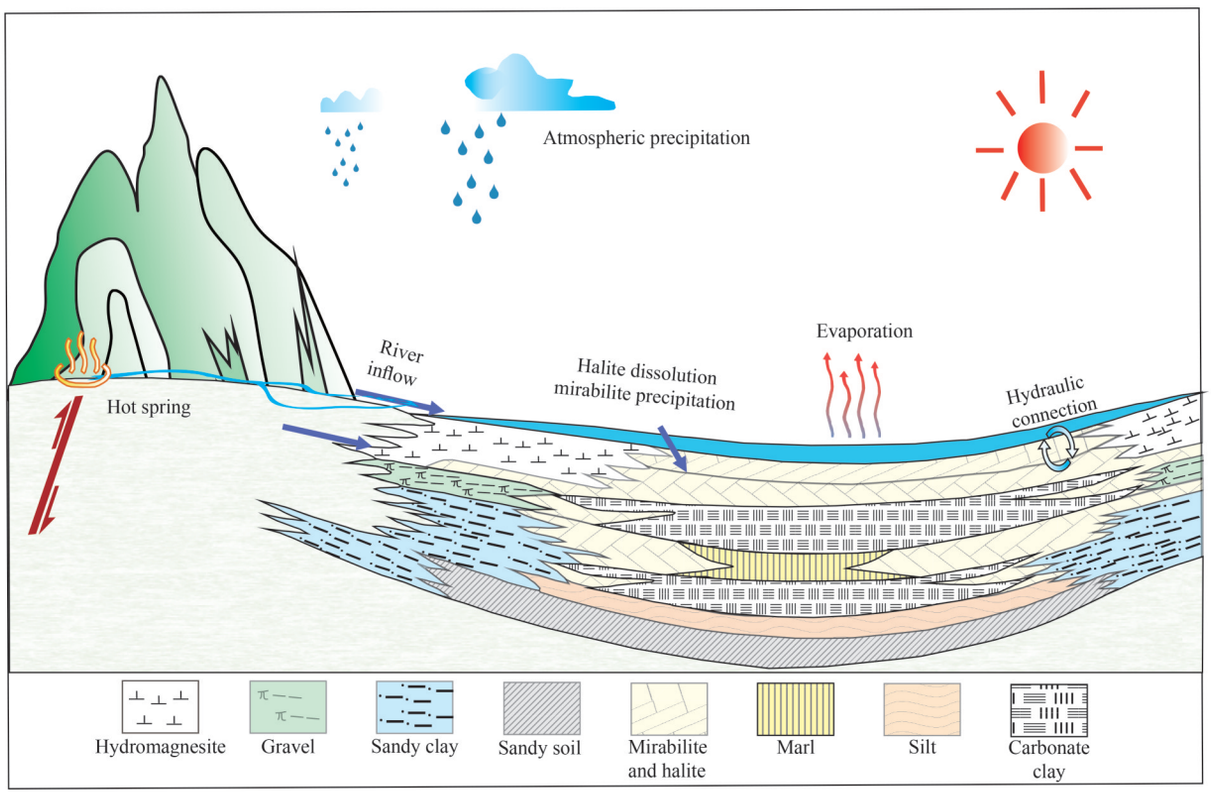

Fig.13 The formation model of the shallow-buried brines in the BCSL

Modified from Zheng et al., 2002.

hydrochemistry and formation mechanisms of these shallow-buried brines, leading to the following conclusions:

(1) The shallow-buried brines exhibited high pH, TDS and are characterized by high Na^+, Cl^-, SO_4^{2-}, CO_3^{2-} and K^+, low Ca^{2+}, Mg^{2+}, Li^+, B^{3+}, and Br^- are substantially higher than the industrial demands, indicating considerable resource potential.

(2) The shallow-buried brines displayed notable spatial heterogeneity, where high-concentration zones were predominantly found in the southern portion of Lake II and the central area of Lake III (TDS>300 g/L). In contrast, peripheral regions, such as river inflow zones, were markedly influenced by freshwater dilution (TDS<60 g/L), thereby offering valuable spatial guidance for resource exploration and development.

(3) Hydrogen and oxygen isotopes revealed that the shallow-buried brines were originated from evaporated meteoric waters. Some brines might be influenced by surrounding recharge waters or diluted lake brines.

(4) Variations in the Na^+, Cl^-, and SO_4^{2-} concentrations of the shallow-buried brines were primarily controlled by the dissolution or precipitation of halite and mirabilite. Changes in the concentrations of Mg^{2+}, Ca^{2+}, CO_3^{2-}, and HCO_3^- are related to the precipitation of carbonate minerals. Trace Li^+, B^{3+}, and Br^- were sourced from the geothermal waters and concentrate in the brines. During the burial process, boron might precipitate in the form of borates, while Br was released into the brines from the sediments.

(5) The formation of the shallow-buried brines was a complex, multi-stage hydrochemical processes. Evapo-concentration, dissolution and precipitation of salt minerals, water mixing, and burial processes significantly influenced the chemical compositions of the shallow-buried brines.

(6) The shallow-buried brines were genetically derived from lake brines, maintaining their inherited relationship with the parent fluids. Post-burial modification processes, including groundwater mixing, mineral dissolution-precipitation reactions, and water-rock interactions, had affected the distinctive geochemical signatures to the shallow-buried brines while preserving their genetic connection to the original surface lake brines.

7 DATA AVAILABILITY STATEMENT

The datasets generated during and/or analyzed during the current study are available from the corresponding author on reasonable request.

8 ACKNOWLEDGMENT

We thank Xiuzhen MA, Zhe MA, Yuan LI, Fukang YANG, and Jilei YANG from the Qinghai Institute of Salt Lakes, Chinese Academy of Sciences, for their support on field and laboratory work.

References

Craig H. 1961. Isotopic variations in meteoric waters. *Science*, **133**(3465): 1702-1362, https://doi.org/10.1126/science.133.3465.1702.

Cheng H D, Ma H Z, Tan H B et al. 2008. Geochemical characteristics of bromide in potassium deposits: review and research perspectives. *Bulletin of Mineralogy, Petrology and Geochemistry*, **27**(4): 410-418. (in Chinese with English abstract)

Horita J, Gat J R. 1989. Deuterium in the Dead Sea: remeasurement and implications for the isotopic activity correction in brines. *Geochimica et Cosmochimica Acta*, **53**(1): 131-133, https://doi.org/10.1016/0016-7037(89)90279-2.

Jiang P W. 2020. Distribution Characteristics of Boron Contents in Water and Surrounding Rock and Provenance Analysis of Boron-Rich Fluids in the North-Central Margin of Qaidam Basin. University of Chinese Academy of Sciences (Qinghai Institute of Salt Lakes), Xining, https://doi.org/10.27577/d.cnki.gqhyy.2020.000008. (in Chinese with English abstract)

Jiang T M, Ji L M, Cheng H D et al. 2021. Algae mineralization experiment and genetic analysis of hydromagnesite in Bangor Lake, Xizang (Tibet). *Geological Review*, **67**(6): 1709-1726, https://doi.org/10.16509/j.georeview.2021.09.011. (in Chinese with English abstract)

Kapp P, Yin A, Harrison T M et al. 2005. Cretaceous-Tertiary shortening, basin development, and volcanism in central Tibet. *GSA Bulletin*, **117**(7-8): 865-878, https://doi.org/10.1130/B25595.1.

Kim S T, O'Neil J R, Hillaire-Marcel C et al. 2007. Oxygen isotope fractionation between synthetic aragonite and water: influence of temperature and Mg^{2+} concentration. *Geochimica et Cosmochimica Acta*, **71**(19): 4704-4715, https://doi.org/10.1016/j.gca.2007.04.019.

Li B K. 2022. Material Source, Migration Process and Formation Model of Boron-Rich Salt Lake in Qinghai-Tibet Plateau. University of Chinese Academy of Sciences (Qinghai Institute of Salt Lakes), Xining, https://doi.org/10.27577/d.cnki.gqhyy.2022.000001. (in Chinese with English abstract).

Li B K, He M Y, Ma H Z et al. 2022. Boron isotope geochemistry of Bangor Co Salt Lake (central Tibet): implications for boron origin and uneven mixing of lake water. *Acta Geochimica*, **41**(5): 731-740, https://doi.org/10.1007/s11631-022-00542-1.

Li S Q, Ye C Y, Zhao Y Y. 2024. Analysis of inter-monthly variation and driving factors of water level fluctuation in Bankog Co, a Lithium-Rich Salt Lake, central Tibetan Plateau. *Acta Geoscientica Sinica*, **45**(5): 691-705, https://doi.org/10.12119/j.yhyj.202401005. (in Chinese with English abstract)

Li S Q, Ye C Y, Zhao Y Y et al. 2025. Quantitative estimation of Li, Rb, Cs sources and its metallogenic significance in the brine lithium deposits in the Tibetan Plateau: a case study of Dangxiong Co. *Acta Petrologica Sinica*, **41**(3): 995-1013, https://doi.org/10.18654/1000-0569/2025.03.15. (in Chinese with English abstract)

Liu C L, Yu X C, Yuan X Y et al. 2021a. Characteristics, distribution regularity and formation model of brine-type Li deposits in salt lakes in the world. *Acta Geologica Sinica*, **95**(7): 2009-2029, https://doi.org/10.19762/j.cnki.dizhixuebao.2021230. (in Chinese with English abstract)

Liu K, Ke L H, Wang J D et al. 2021b. Ongoing drainage reorganization driven by rapid lake growths on the Tibetan Plateau. *Geophysical Research Letters*, **48**(24): e2021GL095795, https://doi.org/10.1029/2021GL095795.

Liu M L, Zheng A T, Shang J B et al. 2023. Progress in study of boron geochemistry in high temperature geothermal fluids. *Earth Science*, **48**(3): 878-893, https://doi.org/10.3799/dqkx.2022.235. (in Chinese with English abstract)

Lü P, Qu Y G, Li Q W et al. 2003. Shelincuo and Bangecuo extensional lake basins in the northern part of Tibet and present chasmic activities. *Jilin Geology*, **22**(2): 15-19, https://doi.org/10.3969/j.issn.1001-2427.2003.02.002. (in Chinese with English abstract)

Niu X S, Liu X F, Lü Y Y et al. 2023. Origin mechanism of thermal springs and their supply of minerals to the salt lake (Li-Rb-Cs) in the Tangqung Co watershed of Tibet. *Geology in China*, **50**(4): 1163-1175, https://doi.org/10.12029/gc20220527001. (in Chinese with English abstract)

Shi Z W, Tan H B, Xue F et al. 2024. Hydrochemical evolution and source mechanisms governing the unusual lithium and boron enrichment in salt lakes of northern Tibet. *GSA Bulletin*, **136**(11-12): 5174-5190, https://doi.org/10.1130/B37516.1.

Stewart M K. 1974. Hydrogen and oxygen isotope fractionation during crystallization of mirabilite and ice. *Geochimica et Cosmochimica Acta*, **38**(1): 167-172, https://doi.org/10.1016/0016-7037(74)90201-4.

Taylor H P. 1974. The application of oxygen and hydrogen isotope studies to problems of hydrothermal alteration and ore deposition. *Economic Geology*, **69**(6): 843-883, https://doi.org/10.2113/gsecongeo.69.6.843.

Tibet Zhongxin Investment Co., Ltd. 2024. Report on resource reserve verification of magnesite, lithium-boron-potassium mineral resources in Bankog Co Salt Lake, Bange County, Tibet Autonomous Region. Unpublished internal report. (in Chinese with English

abstract)

Wang C G, Zheng M P, Zhang X F et al. 2020. Geothermal-type lithium resources in Southern Tibetan Plateau. *Science & Technology Review*, **38**(15): 24-36, https://doi.org/10.3981/j.issn.1000-7857.2020.15.003. (in Chinese with English abstract)

Yan L J, Zheng M P, Wei L J. 2016. Change of the lakes in Tibetan Plateau and its response to climate in the past forty years. *Earth Science Frontiers*, **23**(4): 310-323, https://doi.org/10.13745/j.esf.2016.04.027. (in Chinese with English abstract)

Yang J L, Li X, Lü D et al. 2025. Hydrological changes and their effects on the enrichment of boron andlithium resources in Selin Co-Bangor Co. *Journal of Salt Lake Research*, published OnlineFirst, September 2025, https://doi.org/10.3724/j.yhyj.2025016. (in Chinese with English abstract)

Yang Y H, Weng B S, Yan D H et al. 2021. Tracing potential water sources of the Nagqu River using stable isotopes. *Journal of Hydrology*: *Regional Studies*, **34**: 100807, https://doi.org/10.1016/j.ejrh.2021.100807.

Yin A, Harrison T M. 2000. Geologic evolution of the Himalayan-Tibetan orogen. *Annual Review of Earth and Planetary Sciences*, **28**: 211-280, https://doi.org/10.1146/annurev.earth.28.1.211.

Yu H X, Li Q K, Du Y S et al. 2024. Distribution characteristics and possible sources of bromine in salt lakes on the Qinghai-Xizang Plateau. *Journal of Lake Sciences*, **36**(3): 827-835, https://doi.org/10.18307/2024.0329. (in Chinese with English abstract)

Zhang P X. 1987. Salt Lakes in Qaidam Basin. Science Press, Beijing, 235p. (in Chinese with English abstract)

Zhao G T, Du Y S, Wei H C et al. 2018. Optically stimulated luminescence dating of paleo-shorelines of Bange Co, Qinghai-Tibetan Plateau and its implications for palaeo-environment. *Journal of Salt Lake Research*, **26**(3): 26-34, https://doi.org/10.12119/j.yhyj.201802005. (in Chinese with English abstract)

Zhao X T, Zhao Y Y, Zheng M P et al. 2011. Late quaternary lake development and denivellation of Bankog Co as well as lake evolution of southeastern north Tibetan Plateau during the last great lake period. *Acta Geoscientica Sinica*, **32**(1): 13-26, https://doi.org/10.3975/cagsb.2011.01.03. (in Chinese with English abstract)

Zhao Y Y, Zhao X T, Zheng M P et al. 2006. The denivellation of Bankog Co in the past 50 years, Tibet. *Acta Geologica Sinica*, **80**(6): 876-884, https://doi.org/10.3321/j.issn:0001-5717.2006.06.009. (in Chinese with English abstract)

Zheng M P, Liu X F. 2010. Hydrochemistry and minerals assemblages of salt lakes in the Qinghai-Tibet Plateau, China. *Acta Geological Sinica*, **84**(11): 1585-1600, https://doi.org/10.19762/j.cnki.dizhixuebao.2010.11.005. (in Chinese with English abstract)

Zheng M P, Liu X F. 2009. Hydrochemistry of salt lakes of the Qinghai-Tibet Plateau, China. *Aquatic Geochemistry*, **15**(3): 293-320. https://doi.org/10.1007/s10498-008-9055-y. (in Chinese with English abstract)

Zheng M P, Xiang J, Wei X J et al. 1989. Saline Lakes on the Qinghai-Xizang (Tibet) Plateau. Beijing Science and Technology Publishing, Beijing. 411p. (in Chinese)

Zheng M P, Zhang Y S, Liu X F et al. 2016. Progress and prospects of salt lake research in China. *Acta Geologica Sinica*, **90**(9): 2123-2166, https://doi.org/10.3969/j.issn.0001-5717.2016.09.004. (in Chinese with English abstract)

Zheng X Y, Zhang M G, X C et al. 2002. Records of Salt Lakes in China. Science Press, Beijing. 414p. (in Chinese with English abstract)

Zhou J D, Li B K, He M Y et al. 2023. Hydrochemical characteristics and sources of lithium in carbonate-type salt lake in Tibet. *Sustainability*, **15**(23): 16235, https://doi.org/10.3390/su152316235.

Electronic supplementary material

Supplementary material (Supplementary Table S1 and Figs.S1–S2) is available in the online version of this article at https://doi.org/10.1007/s00343-025-5187-9.